Antifungal activity and mechanism of novel peptide GmAMP against fluconazole-resistant *Candida tropicalis* (#107228)

First submission

Guidance from your Editor

Please submit by 5 Dec 2024 for the benefit of the authors (and your token reward) .



Structure and Criteria

Please read the 'Structure and Criteria' page for guidance.



Custom checks

Make sure you include the custom checks shown below, in your review.



Raw data check

Review the raw data.



Image check

Check that figures and images have not been inappropriately manipulated.

If this article is published your review will be made public. You can choose whether to sign your review. If uploading a PDF please remove any identifiable information (if you want to remain anonymous).

Files

Download and review all files from the <u>materials page</u>.

Q Custom checks

6 Figure file(s)

8 Table file(s)

DNA data checks

- Have you checked the authors <u>data deposition statement</u>?
- Can you access the deposited data?
- Has the data been deposited correctly?
- Is the deposition information noted in the manuscript?

Cell line checks

Is the correct provenance of the cell line described?

Structure and Criteria



Structure your review

The review form is divided into 5 sections. Please consider these when composing your review:

- 1. BASIC REPORTING
- 2. EXPERIMENTAL DESIGN
- 3. VALIDITY OF THE FINDINGS
- 4. General comments
- 5. Confidential notes to the editor
- You can also annotate this PDF and upload it as part of your review

When ready submit online.

Editorial Criteria

Use these criteria points to structure your review. The full detailed editorial criteria is on your guidance page.

BASIC REPORTING

- Clear, unambiguous, professional English language used throughout.
- Intro & background to show context.
 Literature well referenced & relevant.
- Structure conforms to <u>PeerJ standards</u>, discipline norm, or improved for clarity.
- Figures are relevant, high quality, well labelled & described.
- Raw data supplied (see <u>PeerJ policy</u>).

EXPERIMENTAL DESIGN

- Original primary research within Scope of the journal.
- Research question well defined, relevant & meaningful. It is stated how the research fills an identified knowledge gap.
- Rigorous investigation performed to a high technical & ethical standard.
- Methods described with sufficient detail & information to replicate.

VALIDITY OF THE FINDINGS

- Impact and novelty is not assessed.

 Meaningful replication encouraged where rationale & benefit to literature is clearly stated.
- All underlying data have been provided; they are robust, statistically sound, & controlled.



Conclusions are well stated, linked to original research question & limited to supporting results.

Standout reviewing tips



The best reviewers use these techniques

Т	p

Support criticisms with evidence from the text or from other sources

Give specific suggestions on how to improve the manuscript

Comment on language and grammar issues

Organize by importance of the issues, and number your points

Please provide constructive criticism, and avoid personal opinions

Comment on strengths (as well as weaknesses) of the manuscript

Example

Smith et al (J of Methodology, 2005, V3, pp 123) have shown that the analysis you use in Lines 241-250 is not the most appropriate for this situation. Please explain why you used this method.

Your introduction needs more detail. I suggest that you improve the description at lines 57-86 to provide more justification for your study (specifically, you should expand upon the knowledge gap being filled).

The English language should be improved to ensure that an international audience can clearly understand your text. Some examples where the language could be improved include lines 23, 77, 121, 128 – the current phrasing makes comprehension difficult. I suggest you have a colleague who is proficient in English and familiar with the subject matter review your manuscript, or contact a professional editing service.

- 1. Your most important issue
- 2. The next most important item
- 3. ...
- 4. The least important points

I thank you for providing the raw data, however your supplemental files need more descriptive metadata identifiers to be useful to future readers. Although your results are compelling, the data analysis should be improved in the following ways: AA, BB, CC

I commend the authors for their extensive data set, compiled over many years of detailed fieldwork. In addition, the manuscript is clearly written in professional, unambiguous language. If there is a weakness, it is in the statistical analysis (as I have noted above) which should be improved upon before Acceptance.



Antifungal activity and mechanism of novel peptide GmAMP against fluconazole-resistant *Candida tropicalis*

Ruxia Cai $^{Equal \, first \, author, \, 1}$, Na Zhao $^{Equal \, first \, author, \, 1, \, 2}$, Chaoqin Sun 1 , Mingjiao Huang $^{1, \, 3}$, Zhenlong Jiao $^{1, \, 3}$, Jian Peng $^{1, \, 2}$, Jin Zhang 4 , Guo Guo $^{Corresp. \, 1, \, 2}$

Corresponding Author: Guo Guo Email address: guoguojsc@163.com

Background. The overusing of antifungal drugs leads to an increase in the number of clinically isolated fluconazole-resistant Candida spp. so it is an urgent need to develop novel alternative therapeutic strategies. GmAMP is a novel peptide screened by us using artificial intelligence modeling techniques, and pre-tests showed its strong antimicrobial activity against clinically fluconazole-resistant Candida tropicalis. Methods. The study aimed to comprehensively investigate the antimicrobial activity and mechanisms of GmAMP against fluconazole-resistant C. tropicalis. The antifungal activity of GmAMP against fluconazole-resistant C. tropicalis was measured by broth microdilution method, growth and fungicidal kinetics, hypha transformation, and antibiofilm assay. To further uncover the potential mechanisms of action of GmAMP, we performed scanning electron microscopy, flow cytometry, cell membrane potential probe DiSC3(5), and reactive oxygen species probe DCFH-DA detection to assess the cellular morphology and structure, membrane permeability, membrane depolarization, and ROS accumulation, respectively. At the same time, we evaluated the toxicity of GmAMP in vitro through erythrocyte hemolysis degree and cytotoxicity assays. Cytotoxicity and therapeutic efficacy in vivo were assessed by the Galleria mellonella larvae infection model. Results. GmAMP exhibited significant antifungal activity against fluconazole-resistant C. tropicalis with a MIC of 25 µM and demonstrated fungicidal effects at 100 µM within 2 h. inhibited the transition from yeast to hypha morphology, restrained the biofilm formation rate of 88.32%, and eradicated the mature biofilm rate of 58.28%. Furthermore, treatment of fluconazoleresistant C. tropicalis with GmAMP at a concentration of 100 µM resulted in cell structure damage while treatment with GmAMP at concentrations ranging from 25 \sim 100 μ M all caused membrane permeability, depolarization of cell membrane potential, and

¹ School of Basic Medical Sciences, Guizhou Key Laboratory of Microbial and Infectious Disease Prevention & Control, Guizhou Medical University, Guiyang, Guizhou, China

² Key Laboratory of Environmental Pollution Monitoring and Disease Control (Guizhou Medical University), Ministry of Education,, Guiyang, Guizhou, China

³ Translational Medicine Research Center, Guizhou Medical University, Guiyang, Guizhou, China

⁴ School of Public Health, Guizhou Medical University, Guiyang, Guizhou, China



intracellular ROS accumulation, Moreover, GmAMP enhanced the survival rate of 75% for G. mellonella with fluconazole-resistant C. tropicalis infection as well as reduced fungal burden in vivo by approximately 1.0×102 CFU per larva. Conclusion. GmAMP can disrupt the cell membrane of fluconazole-resistant C. tropicalis and also shows favorable safety and therapeutic efficacy in vivo. Accordingly, GmAMP has the potential to be an agent against drug-resistant fungi.



1 Antifungal activity and mechanism of novel peptide GmAMP against

2 fluconazole-resistant Candida tropicalis

- 3 Ruxia Cai ¹, Na Zhao ^{1, 2}, Chaoqin Sun ¹, Mingjiao Huang ^{1, 3}, Zhenlong Jiao ^{1, 3}, Jian Peng ^{1, 2},
- 4 Jin Zhang ⁴, Guo Guo ^{1, 2}
- ⁵ School of Basic Medical Sciences, Guizhou Key Laboratory of Microbial and Infectious
- 6 Disease Prevention & Control, Guizhou Medical University, Guiyang, 550025, China.
- ⁷ Key Laboratory of Environmental Pollution Monitoring and Disease Control (Guizhou Medical
- 8 University), Ministry of Education, Guiyang, 561113, China.
- ⁹ Translational Medicine Research Center, Guizhou Medical University, Guiyang, 561113,
- 10 China.
- ⁴ School of Public Health, Guizhou Medical University, Guiyang, 561113, China.

12 Correspondence Author:

- 13 Guo Guo 1, 2
- Building Wuben, School of Basic Medical Sciences, Guizhou Medical University, Gui'an New
- District, Guiyang, 561113, China.
- 16 **Email address:** guoguojsc@163.com



ABSTRACT

- 18 **Background.** The overusing of antifungal drugs leads to an increase in the number of clinically
- isolated fluconazole-resistant *Candida* spp. so it is an urgent need to develop novel alternative
- therapeutic strategies. GmAMP is a novel peptide screened by us using artificial intelligence
- 21 modeling techniques, and pre-tests showed its strong antimicrobial activity against clinically
- 22 fluconazole-resistant Candida tropicalis.
- 23 **Methods.** The study aimed to comprehensively investigate the antimicrobial activity and
- 24 mechanisms of GmAMP against fluconazole-resistant C. tropicalis. The antifungal activity of
- 25 GmAMP against fluconazole-resistant *C. tropicalis* was measured by broth microdilution
- method, growth and fungicidal kinetics, hypha transformation, and antibiofilm assay. To further
- 27 uncover the potential mechanisms of action of GmAMP, we performed scanning electron
- 28 microscopy, flow cytometry, cell membrane potential probe $DiSC_3(5)$, and reactive oxygen
- 29 species probe DCFH-DA detection to assess the cellular morphology and structure, membrane
- permeability, membrane depolarization, and ROS accumulation, respectively. At the same time,
- we evaluated the toxicity of GmAMP in vitro through erythrocyte hemolysis degree and
- 32 cytotoxicity assays. Cytotoxicity and therapeutic efficacy in vivo were assessed by the Galleria
- 33 *mellonella* larvae infection model.
- Results. GmAMP exhibited significant antifungal activity against fluconazole-resistant C.
- tropicalis with a MIC of 25 μM and demonstrated fungicidal effects at 100 μM within 2 h.
- inhibited the transition from yeast to hypha morphology, restrained the biofilm formation rate of
- 88.32%, and eradicated the mature biofilm rate of 58.28%. Furthermore, treatment of



- fluconazole-resistant *C. tropicalis* with GmAMP at a concentration of 100 μM resulted in cell
- structure damage while treatment with GmAMP at concentrations ranging from $25 \sim 100 \mu M$ all
- caused membrane permeability, depolarization of cell membrane potential, and intracellular ROS
- accumulation, Moreover, GmAMP enhanced the survival rate of 75% for G. mellonella with
- fluconazole-resistant C. tropicalis infection as well as reduced fungal burden in vivo by
- approximately 1.0×10² CFU per larva.
- 44 Conclusion. GmAMP can disrupt the cell membrane of fluconazole-resistant C. tropicalis and
- also shows favorable safety and therapeutic efficacy in vivo. Accordingly, GmAMP has the
- potential to be an agent against drug-resistant fungi.
- 47 **Keywords:** Antimicrobial peptide; GmAMP; Drug-resistance; Antifungal activity; Candida
- 48 tropicalis
- 49 **INTRODUCTION**
- Opportunistic fungal pathogens can cause cutaneous infections and invasive infections, leading
- to substantial illness and death (Thomas-Rüddel et al. 2022). Among these pathogens, invasive
- candidiasis emerges as a prominent concern, characterized by mortality rates exceeding 40%
- (Sasani et al. 2021; Tsay et al. 2020). C. tropicalis is a part of the human microbiomes but is also
- capable of causing invasive infection and it is widely regarded as the second to fourth most
- virulent genus of *Candida* species (Contreras Martínez et al. 2022). Azole antifungal agents,
- including fluconazole, itraconazole, voriconazole, posaconazole, and others, constitute the
- 57 primary therapeutic resources against *C. tropicalis* infection. However, the indiscriminate and
- excessive use of azoles has engendered the emergence of azole-resistant strains of *C. tropicalis*



- from clinical isolates. In addition, epidemiologic studies have shown that *C. tropicalis* has a
- 60 higher rate of resistance to fluconazole compared to other *Candida* species (Tseng et al. 2022).
- 61 Consequently, invasive infection due to high rates of azole resistance in *C. tropicalis* clinical
- 62 isolates has attracted increasing attention (Fan et al. 2023). In 2022, the World Health
- Organization (WHO) issued the first list of fungal priority pathogens aimed at developing a
- 64 strategic framework for research, development, and public health interventions, with C.
- 65 tropicalis listed as a high-priority pathogen (Fisher & Denning 2023; World Health Organization
- 66 (WHO) 2022).
- 67 It is widely recognized that azoles, especially fluconazole, are crucial therapeutic and protective
- agents for the controlling of *Candida* infections. However, due to the frequent and widespread
- use of fluconazole, there is an increasing trend of resistance, which eventually leads to the
- emergence of cross-resistance to other antifungal compounds (Chai et al. 2010; Jia et al. 2019;
- Pappas et al. 2016). Studies have shown that resistance rates of *C. tropicalis* to azoles such as
- fluconazole, itraconazole, voriconazole, and posaconazole have recorded resistance rates as high
- as 40% to 80% (World Health Organization (WHO) 2022). In addition, more than 21% of C.
- 74 tropicalis isolates in China are resistant to fluconazole and even 21.7% of *C. tropicalis* isolates
- were two to four times more resistant to multi-azoles in Iran (Badiee et al. 2022; Liu et al. 2022).
- 76 This resistance phenomenon may stem from various factors, including alterations in drug targets,
- vpregulation of drug target expression, and increased expression of efflux pumps (Lee et al.
- 78 2021). As a result, antifungal drug therapies may be inefficient in treating drug-resistant
- candidiasis, which poses significant challenges in clinical management (McCarthy & Walsh



well as alternative therapeutic approaches is essential to address the current problem of fungal 81 drug resistance. 82 Antimicrobial peptides (AMPs) represent critical components of the immune defense system in 83 organisms, with broad-spectrum antimicrobial activity, low drug resistance, and diverse 84 bactericidal mechanisms (Li et al. 2020). The mechanism by which antimicrobial peptides 85 interact with cell membranes to fulfill their antimicrobial and bactericidal effects has long been 86 accepted (Fernández de Ullivarri et al. 2020; Zhou et al. 2023). This unique mechanism makes it 87 not easily susceptible to the development of resistance. In earlier period research work, We 88 employed multitasking adaptive modeling and model adaptation to establish a prediction model 89 and screening protocol for antifungal peptides based on antimicrobial peptide databases such as 90 APD, DRAMP, CAMP, antifp, etc (Zhang et al. 2022). Then we predicted more than three 91 million unknown functional sequences in the UniProt database from the established model and 92 screened out several hundreds of peptides that might be antifungally active then synthesized 93 them by solid-phase organic synthesis method, and the antimicrobial activity was verified by wet 94 95 showed strong antimicrobial activity against fluconazole-resistant C. tropicalis in the pre-test, 96 with a MIC of 25 μ M (MIC of fluconazole against this isolate >3343 μ M). 97

2017; Zhang et al. 2017). Therefore, the exploitation of novel and potential antifungal agents as

- According to the sequence homology nomenclature in the antimicrobial peptide APD3 database (http://aps.unmc.edu/AP/, main.html), The novel peptide was named GmAMP. To more fully
- assess GmAMP, we first determined the MIC of GmAMP against four strains of clinically



fluconazole-resistant *C. tropicalis* and the standard strain of *C. tropicalis* ATCC 20962, for which GmAMP showed excellent antimicrobial activity. Besides, to assess the antifungal activity and mechanism of GmAMP, we performed experimental validation on fluconazole-resistant *C. tropicalis*. As a result, the antifungal mechanism of GmAMP against fluconazole-resistant *C. tropicalis* was investigated in terms of physicochemistry and morphology, and its in vivo efficacy was evaluated by the *G. mellonella* larvae infection model. Thus, the findings of this study provide a certain experimental basis for the exploration and utilization of novel peptide antimicrobial drugs.

MATERIALS AND METHODS

Materials

- - Strains and cell culture conditions
- The fluconazole-resistant *C. tropicalis* 4171, 4252, 6984, and 8402 were collected from infected patient's blood in the affiliated hospital of Guizhou Medical University. *C. tropicalis* ATCC 20962 was purchased from the Shanghai Conservation Biotechnology Center. All strains were grown in yeast extract peptone dextrose medium (YPD, Solarbio, Beijing, China) at 35°C with



shaking at 200 rpm until the cultures reached the exponential growth phase. RPMI-1640 122 (Invitrogen, Carlsbad, CA, United States) supplemented with 15% fetal bovine serum (FBS) 123 (Sigma-Aldrich) was used as the culture medium for hypha growth of C. tropicalis. The mouse 124 monocyte-macrophage cell line RAW 264.7 was donated by Jiahong Wu from the Key and 125 Characteristic Laboratory of Modern Pathogen Biology, Guizhou Medical University, and cells 126 were cultured in DMEM medium (Gibco, USA) containing 10% fetal bovine serum (FBS, 127 Gibco, USA), 100 U/mL penicillin (Gibco, USA), and 100 μg/mL streptomycin (Gibco, USA) 128 and maintained at 37°C in a humidified 5% CO2 incubator. 129 **Antifungal Activity** 130

The minimum inhibitory concentration (MIC) of GmAMP for four fluconazole-resistant C. 131 tropicalis from clinical isolates, a standard strain of C. tropicalis ATCC 20962 was determined 132 by using broth microdilution method according to the Standards of Clinical and Laboratory 133 Standards Institute (CLSI) (CLSI Clinical and Laboratory Standards Institute; 2023). In brief, 134 these yeasts of fungal strains were cultured in YPD broth medium at 35°C to the logarithmic 135 growth stage, and the cultures were washed by phosphate-buffered saline (PBS, 10 mM, pH 7.4) 136 three times and resuspension to $0.5 \times 10^3 \sim 2.5 \times 10^3$ CFU/mL. Then 100 μ L above fungal 137 suspension was added to a 96-well plate with a series concentration of GmAMP and fluconazole 138 (Yuan ye, Shanghai, China) and co-cultured with fungal suspension at 35°C for 24 h, and 10 mM 139 PBS and medium were used as the negative and blank controls, respectively. The drug 140 141 concentration corresponding to the well without visible fungal growth was regarded as MIC and the experiment was performed in triplicate and repeated three times. 142



156

Growth and fungicidal kinetics

To analyze the antifungal or fungicidal process of GmAMP against fluconazole-resistant C. 144 tropicalis, the growth kinetics and time-kill kinetics of GmAMP on fluconazole-resistant C. 145 tropicalis were further investigated at different times after GmAMP treatment as to previously 146 described (Melo et al. 2024). The concentration of the prepared fungal cells was 1.0×10^6 147 CFU/mL according to the previously mentioned method and incubated with 25, 50, and 100 µM 148 of GmAMP at 35°C for 48 h. During co-culture, the OD_{630nm} was recorded every 2 h by a 149 microplate reader (Thermo Scientific, USA). Meanwhile, the cultured yeasts were taken at 150 specific time intervals (0, 2, 4, 6, 8, 10, 12 h), then the agar solid plate experiment was 151 carried out after gradient dilution, and 10 mM PBS and medium was used as the negative and 152 blank controls in the experiment. Fungal colonies were counted after incubation at 35°C for 24 h. 153 Finally, the results were presented as the average of triplicate measurements from three 154 independent assays. 155

Effect of GmAMP on hypha formation

To analyze the effect of GmAMP on the transition of yeast-to-hyphal phase in fluconazoleresistant *C. tropicalis* as described previously (Lochenie et al. 2024). The concentration of the
prepared fungal cells was 1.0×10⁶ CFU/mL in RPMI 1640 medium (Gibco, USA) which
contained 15% fetal bovine serum (Gibco, USA) according to the previously mentioned method.
Then 500 μL of fungal suspension was incubated with GmAMP at concentrations (25, 50, and
100 μM) in 24 well plates and 10 mM PBS as the negative control. Next the plate after
cultivation at 37 °C for 3, 6, 9, 12, and 24 h, the hypha formation was observed and



photographed under an inverted microscope.

Antibiofilm Assay

The fungal cells cultured to logarithmic phase were adjusted to 1.0×10⁶ CFU/mL by using 166 RPMI-1640 liquid medium and were added to the 96-well polypropylene plate and then 167 incubated at 37°C for 90 mins (early biofilm formation) or 48 h (mature biofilm formation) 168 according to previous method (Zou et al. 2024). And 100 µL newly prepared 2,3-bis(2-methoxy-169 4-nitro-5-sulfophenyl) 2H-tetrazolium5-carboxamide sodium salt (XTT) solution (Yuan ye, 170 Shanghai, China) was added to each well for 2 h at 37°C after different concentrations of 171 GmAMP were added and continued to co-incubate for 24 h. Absorbance was measured by using 172 a microplate reader at OD_{490nm}. Next, the sterile poly-lysine cell crawling tablets were placed at 173 the bottom of the 24-well plate, and fungal suspension with the above concentration of 500 µL 174 was added. The early and mature biofilms were prepared according to the XTT method, and 500 175 μL of SYTO 9 (Invitrogen, USA) and propidium iodide (PI, Sigma, USA) solution with the final 176 concentration of 10 µM were added and incubated for 20 mins while 10 mM PBS was used as 177 the negative control. Using nail polish to seal the cover glass, laser confocal microscopy was 178 used to observe and obtain images. 179

Scanning electron microscope

180

181

182

183

184

The concentration of the prepared fungal cells was 1.0×10⁶ CFU/mL based on the previous description with minor modifications (Alfaro-Vargas et al. 2022), incubated in GmAMP with culture medium at 35°C for 2 h, and 10 mM PBS was used as the negative control, then the suspension was centrifuged at 5000 rpm for 10 mins, fixed with 2.5% glutaraldehyde overnight



195

202

at 4°C, and dehydrated with 50%, 75%, 95% and 100% series of ethanol solutions for 10 minutes. It was then dried in a vacuum evaporator and coated with a thin layer of goldpalladium. The samples were observed by scanning electron microscopy and the image acquisition was performed using a Hitachi Regulus SU8100 (Tokyo, Japan)

Flow cytometry analysis

The concentration of the prepared fungal cells was 1.0×10^6 CFU/mL according to the previous description with minor modifications (Torres et al. 2023), GmAMP with different concentrations was incubated at 35°C for 1 h, and 10 mM PBS was used as the negative control. After that, the fungal suspension was incubated with SYTO 9 and PI staining with a final concentration of 10 μ M at 35°C for 15 mins, and the stained cells were analyzed by flow cytometry.

Membrane potential

The concentration of the prepared fungal cells was 1.0×10⁶ CFU/mL as described in the previous study (Decker et al. 2024), then added to 96-well plates while the membrane potential DiSC₃(5) probe was added into the fungal suspension, then treated with different concentrations of GmAMP as well as 10 mM PBS was used as the negative control to be measured fluorescence intensity. The change of fluorescence intensity in 1 h was continuously and dynamically monitored with by RF-5301PC sectrofluoro-photometer (Bio-Tek Synergy HTX, United States).

Reactive oxygen species level

The levels of ROS were determined by using 2', 7'-dichlorodihydrofluorescein diacetate (DCFH-DA, Yuan ye, Shanghai, China) according to previously described with minor modifications

(Shaban et al. 2024). The 1.0×10^6 CFU/mL of fungal suspension was incubated with $10~\mu M$



DCFH-DA, and PBS was used as the negative control. The change of fluorescence intensity in 1
h was continuously and dynamically monitored by RF-5301PC sectrofluoro-photometer (BioTek Synergy HTX, United States).

Cytotoxicity Assays

Mouse RAW 264.7 cells were used to evaluate the cytotoxicity of GmAMP on mammalian cells 210 as previously described (de Oliveira et al. 2023). Cells were cultured in Dulbecco's Modified 211 Eagle Medium (DMEM, Gibco, Grand Island, NY, USA) containing 10% fetal bovine serum 212 (FBS, Gibco, USA), 1% penicillin-streptomycin (Gibco, USA), and maintained at 37°C in a 213 humidified 5% CO₂ incubator. Firstly, 100 µL of RAW 264.7 cells suspension (2×10⁴ cells/mL) 214 was added to 96-well plates for cultivating overnight. 100 µL with different concentrations of 215 GmAMP solution was added and then incubated at 37°C for 24 h. 10 mM PBS and complete 216 medium were used as the negative and blank controls, respectively. After the end of incubation, 217 10 μL of CCK8 solution was added to each assay well and incubated for 1 h. Absorbance values 218 were detected at OD_{450nm} and the percentage of cell survival was counted. 219

220

Cell viability(%) =
$$(\frac{Abs_{450nm} of GmAMP solution - Abs_{450nm} of blank control}{Abs_{450nm} of PBS control - Abs_{450nm} of blank control}) \times 100\%$$

222

223

Hemolysis of Human Red Blood Cells

- The human red blood cells (hRBCs) were used to evaluate the hemolytic activity of GmAMP on
- 225 the basis of previous descriptions with minor modifications (Chiramba et al. 2024). The



GmAMP with different concentrations and 2% hRBCs were added to the 96-well plate and incubated for 1 h in 37°C. 1% Triton X-100 (Solarbio, Beijing, China) was the positive control, and 10 mM PBS was used as the negative control. After the end of incubation, the samples were taken out and centrifuged at 1000 rpm for 10 min, the supernatant of samples was transferred to a new 96-well plate, and the percentage of hemolysis was calculated by the OD_{540nm} absorbance value.

Hemolysis(%) =
$$(\frac{Abs_{540nm} \text{ of GmAMP solution} - Abs_{540nm} \text{ of PBS control}}{Abs_{540nm} \text{ of (TritonX} - 100) - Abs_{540nm} \text{ of PBS control}}) \times 100\%$$

Galleria mellonella infection model

The larvae used in the experiment were purchased from Huiyude Biotechnology Co., Ltd., (Tianjin, China), each weighing 250~300 mg and about 2~3 cm in length. As previously described with slight modifications (Fernandes et al. 2020). All larvae were placed in a dark incubator at 35°C overnight before the experiment. Ten larvae were randomly divided into each group to inject 10 μ L of GmAMP solution with a concentration of 8~32 mg/kg into the last left proleg of larvae to evaluate the toxicity of GmAMP. The negative control was given an equal volume of sterile PBS. To evaluate the efficacy of GmAMP, 12 larvae were randomly divided into each group and injected 10 μ L into the last left proleg of larvae with approximately 5.0×10⁸ CFU/mL of fungal suspension. After 1 h in the incubator, the same volume of GmAMP was injected into the last right proleg using the same method. Incubated at 35°C for 5 days, live and



246	dead counts were performed every 24 h, and larvae were considered dead when they turned black
247	or soft and had no obvious tactile response. 24 h after injection of GmAMP, 3 larvae were
248	randomly selected from each group and placed in a 1.5 mL sterile PBS solution for high-speed
249	homogenization grinding. 10 μL of gradient dilution was followed by dripping on a sterile solid
250	YPD plate for culturing 24 h. The number of fungal single colony was recorded, and the <i>C</i> .
251	tropical burden of each larva was counted.
252	Data processing
253	Statistical mapping and data analysis were performed using GraphPad Prism 8.0 software
254	(GraphPad, Software). Data were expressed as mean \pm SD and analyzed by One-Way ANOVA.
255	Long-rank test was used for the analysis of Mantel-Cox survival curves for the G. mellonella
256	survival experiment. The $P < 0.05$ was considered statistically significant.
257	
258	RESULTS
259	GmAMP chemical characteristic
260	The secondary structure of antimicrobial peptides plays an important role in antimicrobial
261	activity. α -helical structure promotes the interaction of antimicrobial peptides with the cell
262	membrane to enhance the antimicrobial activity (Personne et al. 2023). The antimicrobial peptide
263	GmAMP, composed of 21 amino acids, is predicted to have an α -helical structure (Figs. 1A and
264	B). The molecular weight (MW) of GmAMP was confirmed to be 2539.33 Da by mass
265	spectrometry. Furthermore, GmAMP has a net charge of +17 and a hydrophobicity value of -

0.757 (Fig. 1C), and these characteristics suggest that GmAMP is a hydrophilic cationic peptide.

266



Antifungal activity

The results of the antifungal activity assay showed that GmAMP had strong antimicrobial effects 268 against clinical fluconazole-resistant C. tropicalis, with MICs ranging from 25 to 50 μM. In 269 comparison to this, the MIC values of fluconazole against clinical isolates exceeded 3343 µM 270 (Table 1). Consequently, to better understand the effect of GmAMP on fluconazole-resistant C. 271 tropicalis clinical isolate, 4252 isolate (MIC 25 μM) was selected for further study. 272 Growth kinetics and fungicidal kinetics 273 To elucidate the effect of GmAMP on the growth process of fluconazole-resistant *C. tropicalis*. 274 The growth curve of fluconazole-resistant C. tropicalis under GmAMP treatment was further 275 plotted, as shown in Fig. 2A, the fungal cells in the control group entered the logarithmic phase 276 within 6 h and reached the stabilization phase within 18 h. In comparison, GmAMP treatments at 277 concentrations of 25 µM and 50 µM were found to slow down the proliferation rate of 278 fluconazole-resistant C. tropicalis and prolong the time to reach the logarithmic phase. When 279 treated with GmAMP at a concentration of 100 µM, GmAMP showed an inhibitory effect on 280 fluconazole-resistant C. tropicalis and prevented the natural growth and reproduction of 281 fluconazole-resistant C. tropicalis. The time-fungicidal kinetic curve was further plotted to 282 clarify the fungicidal effect of GmAMP (Fig. 2B). Compared with the control group, GmAMP 283 284 exhibited a powerful inhibitory effect on fluconazole-resistant C. tropicalis when the concentrations of GmAMP were 25 µM and 50 µM. Notably, dealing with the concentration at 285 100 μM of GmAMP, the fluconazole-resistant C. tropicalis was killed within 2 h. These results 286 indicate that GmAMP manifests effective antimicrobial activity and fungicidal effect against 287



290

298

299

300

301

302

304

305

306

307

308

288 fluconazole-resistant *C. tropicalis*.

The transformation of yeast to the mycelial phase

Morphological changes during the transformation of the fluconazole-resistant *C. tropicalis* yeast phase to the mycelial phase were observed by using an inverted microscope which is shown in Fig. 2C. The length of the mycelium of the fungus in the control group increased with incubation time, and 9 h of incubation, yeast cells can be seen growing to form bundles of hyphae while forming branches of various sizes and lengths and intertwining with each other to form a net structure, and a more tightly netted biofilm is formed over time. Interestingly, the development of fluconazole-resistant *C. tropicalis* from yeast cells to mycelial morphology was completely

The transformation of *Candida* mycelial morphology is closely related to its pathogenicity.

concentrations of 25 μM and 50 μM not only inhibited morphological transformation but also

inhibited after treatment with different concentrations of GmAMP. GmAMP treatments at

100 uM concentration of GmAMP reduced the number of yeast cells, allowing only a minor

number of yeast cells to be observed. These results suggest that GmAMP inhibited the

morphological transformation process of fluconazole-resistant C. tropicalis from the yeast phase

303 to the mycelial phase.

Inhibition of biofilm formation and eradication of mature biofilm

We visualized the results by using confocal laser scanning microscopy. In the control group of the biofilm formation assay, a compact and intact biofilm was observed to emit predominantly green fluorescence. Nevertheless, after GmAMP treatment, intact biofilms could no longer be formed and only dispersed incomplete membranes of different sizes were observed, while only



310

311

312

313

314

315

316

317

318

319

320

321

322

323

324

325

326

327

328

329

single yeast cells could be seen in the high-concentration group (Fig. 3A). In the control group of the biofilm eradication assay, it was observed that the tightly structured and network-interwoven biofilms mainly emitted green fluorescence. After GmAMP treatment, we found that the tightly structured biofilm became loose and the network structure was reduced and thinned, while a reduction in the number of yeasts and an increase in the number of fungal deaths were observed, with a predominantly red fluorescence (Fig. 3B). In addition, the biofilm activity of C. tropicalis was determined by XTT quantitative method. Compared with the control group, GmAMP at concentrations of 50, 100, and 200 µM inhibited biofilm formation by 49.75%, 71.28%, and 88.32%, respectively (Fig. 3C), and eliminated mature biofilm by 17.53%, 42.07%, and 58.28%, respectively (Fig. 3D). These results indicated that GmAMP inhibited biofilm formation and eradicated a certain amount of mature biofilm in fluconazole-resistant *C. tropicalis*. **Antifungal mechanism** To investigate the impact of GmAMP on the cell morphology of fluconazole-resistant C. tropicalis, the morphological changes induced by GmAMP treatment of fungal cells for 2 h were directly observed by scanning electron microscopy. Untreated fungal cells were morphologically intact, with cell surfaces remaining round and smooth (Fig. 4A). When cells were exposed to 100 μM of GmAMP for 2 h, the cells were destroyed and the surface appeared rough and irregular. (Fig. 4B). Thus, these outcomes suggested that the cellular structural integrity of fluconazoleresistant C. tropicalis has been impaired. To further investigate the interaction of GmAMP on cell membrane of fluconazole-resistant C. tropicalis, PI and SYTO9 fluorescence staining were used to determine the effect of GmAMP on the integrity of cell membrane, PI and STOY9 as



DNA-binding dyes emitted red and green fluorescence, respectively, and the former only 330 penetrated the membrane-damaged cells, while the latter emitted green fluorescence and stained 331 both live and dead cells (Jin et al. 2005). As a result, when cells were exposed to 25, 50, and 100 332 μM of GmAMP, 45.02%, 76.88%, and 85.02% of the cells stained positively for PI, respectively. 333 Moreover, PI staining positivity showed a dose-dependent correlation with GmAMP (Fig. 4C). 334 which indicated that GmAMP disrupted the cell membrane integrity of fluconazole-resistant C. 335 tropicalis. The membrane depolarization was detected using the membrane potential probe 336 DiSC₃(5). As shown in Fig. 4D, compared with the control group, we found that GmAMP 337 treatment caused depolarization of the cell membrane potential of fluconazole-resistant C. 338 tropicalis and the level of membrane potential rose significantly with increasing concentration of 339 GmAMP. Reactive oxygen species (ROS) generally maintain low levels within normal cells, but 340 the accumulation of higher levels of ROS can damage cellular structures (Huang et al. 2020). 341 Here, different concentrations of GmAMP induced ROS accumulation in fluconazole-resistant C. 342 tropicalis, and ROS levels showed a time-dose dependence (Fig. 4E). These results suggest that 343 the presence of GmAMP induced ROS production, which contributed to the crucial factor in the 344 antimicrobial effect of GmAMP. 345 **Hemolytic and Cytotoxicity** 346 To evaluate mammalian cytotoxicity, we assessed the safety of GmAMP on human red blood 347 cells and RAW 264.7 cells. The hemolysis experiment was performed using 2% human red 348 blood cells. At a concentration of 200 µM, GmAMP exhibited slight hemolysis with a hemolysis 349

rate of 35.64% (Fig. 5A). Moreover, GmAMP showed no obvious cytotoxicity to RAW 264.7

350



cells, and the cell viability of mouse macrophage RAW 264.7 remained above 80% at 200 μM concentration of GmAMP (Fig. 5B).

Therapeutic effect on fluconazole-resistant C. tropical infection in vivo

The *Galleria mellonella* larvae infection model was used to study the in vivo therapeutic effect of GmAMP. In the peptide toxicity test (Fig. 6B). All larvae survived and were undead in the experimental model, suggesting that GmAMP did not show significant toxicity in the concentration range of 32 mg/kg. Survival of larvae infected with fluconazole-resistant *C. tropicalis* was increased by injecting various concentrations of GmAMP, with 75% survival in the 32 mg/kg group (*P*<0.05), whereas the control group has 40% survival rate at 5 days post infection (Fig. 6C). These results were also reflected by the fungal burden of *Galleria mellonella* larvae, after treating larvae with GmAMP for 24 hours, and the number of colonies pre larvae was significantly reduced in all treatment groups while 32 mg/kg of GmAMP reduced fungal burden from 5.27×108 to 6.37×106 CFU per larva (Fig. 6D). Consequently, GmAMP has the potential for clinical application as it effectively treats fluconazole-resistant *C. tropicalis* infection and reduces the fungal burden in vivo.

DISCUSSION

Currently, the irrational use of antifungal drugs is leading to a rapid development of resistance to
antifungal drugs resulting in a surge in morbidity and mortality from invasive fungal infection
(Fan et al. 2024). The isolation rate of *Candida* species, such as *Candida albicans*, *Candida*glabrata, *Candida tropicalis*, *Candida krusei*, and *Candida parapsilosis* is steadily increasing in
hospitals (Falagas et al. 2010; Lee et al. 2022). Recent reports show that the proportion of



fluconazole-resistant C. tropicalis isolates continues to rise in China (Wang et al. 2021). The 372 development of new antifungal drugs to address this problem is imminent. Widely distributed in 373 animals, plants, and other organisms, AMPs are a fast and effective barrier against pathogens in 374 humans. AMPs exert their antimicrobial activity through a unique membrane-targeting 375 mechanism that avoids the development of drug resistance and is regarded as a novel alternative 376 to synthetic antibiotics (Mulukutla et al. 2024). 377 In this study, we determined in vitro the antimicrobial activity of GmAMP against four clinical 378 isolates of fluconazole-resistant C. tropicalis and the standard strain of C. tropicalis ATCC 379 20962, and GmAMP showed good antimicrobial effect against clinical isolate of fluconazole-380 resistant C. tropicalis 4252, with a MIC value of 25 µM. GmAMP not only delayed the 381 proliferation rate and inhibited the growth and reproduction of fungi, but also effectively killed 382 GmAMP within 2 h. These results revealed that GmAMP is an effective antimicrobial agent, and 383 there is a need to further investigate the antifungal efficacy of GmAMP. 384 The process of transformation from the yeast phase to the mycelial phase, termed "biphasic", is 385 considered the most important pathogenic characteristic of Candida, and is also recognized as a 386 key stage in biofilm formation and maturation (Zhu et al. 2024). Furthermore, the hyphae formed 387 during the morphological transformation can penetrate cells and invade the bloodstream, 388 expressing a wide range of virulence factors, and are therefore considered to be a more virulent 389 phenotype than yeast (Khamzeh et al. 2023). Herein, GmAMP inhibited the transition of yeast 390 phase cells to mycelial phase morphology, preventing the process of mycelial development, 391 which demonstrates that GmAMP plays a key role in inhibiting the formation and maturation of 392



fluconazole-resistant C. tropicalis biofilm by preventing mycelial development. The yeast cells 393 of C. tropicalis are characterized by a high capacity to form biofilms compared to other Candida 394 species (Zuza-Alves et al. 2017), which may be related to an increased amount of biomass in the 395 membranes and extracellular matrix, leading to a denser structure (Chandra & Mukherjee 2015; 396 Desai & Mitchell 2015). Here, the 50 µM (2×MIC) of GmAMP inhibits biofilm formation and 397 has an eradicative effect on mature biofilms. Moreover, GmAMP inhibited and eliminated 398 biofilms of fluconazole-resistant C. tropicalis in a concentration-dependent manner. Therefore, 399 GmAMP showed good bioactivity in inhibiting morphological transformation and anti-biofilm 400 processes. 401 It has been reported that most antimicrobial peptides exert their antimicrobial effects mainly by 402 targeting cell membranes (Aguiar et al. 2020; Buda De Cesare et al. 2020; Hu et al. 2022). In the 403 present study, the results of the scanning electron microscopy assay demonstrated that GmAMP 404 disrupts the morphology and structure of the fluconazole-resistant C. tropicalis. A similar 405 phenomenon was also found by Ma, et al (Ma et al. 2020; Zhang et al. 2023). Moreover, we 406 speculated the exact reason for the morphological damage and subsequent cell death is correlated 407 with increased membrane permeability resulting from electrostatic interactions between the 408 positively charged peptide GmAMP and the negatively charged components of the fungal 409 cytoplasmic membrane (Boparai & Sharma 2020; Jayasinghe et al. 2023; Kodedová et al. 2019). 410 The experimental result verified membrane permeability by a significant increase in the number 411 of PI-stained positive cells of the fungi treated with GmAMP. Changes in cell membrane 412 permeability usually trigger variation in cell membrane potential, which is closely related to 413



cellular function (D'Auria et al. 2022). When membrane-modifying compounds (e.g., peptides) 414 depolarize the membrane then the potential is lost. DiSC₃(5) is released into the solution, causing 415 fluorescence enhancement, which indicates that the cytoplasmic membrane is altered because of the 416 cell membrane depolarization by the action of GmAMP in a concentration-dependent manner, 417 which suggests that the dissipation of membrane potential might be involved in the formation of 418 channels or pores, then allowed the passage of ions or macromolecules, to lead cytoplasmic 419 membrane dysfunction (Bezerra et al. 2022; Venkatesh et al. 2017). It has been found that aerobic 420 metabolism-generated ROS are usually present in cells that are in equilibrium with antioxidant 421 enzymes, and excess ROS have certain deleterious effects on the basic structure of fungi, such as 422 damage to nucleic acids, DNA, amino acid residues, and cell membranes (Perrone et al. 2008). We 423 found that GmAMP induced the accumulation of reactive oxygen species in a dose-dependent 424 manner (Taveira et al. 2022). In brief, we hypothesized that the cationic peptide GmAMP can interact 425 with certain negatively charged substance molecules on the cell membrane through electrostatic 426 interactions, it leads to a series of consequences such as increased membrane permeability, altered 427 depolarization of the membrane potential, structural loss of membrane integrity, accumulation of ROS, 428 and further leakage of intracellular contents, which finally leads to cytoplasmic membrane dysfunction 429 and cell death. 430 The excellent antimicrobial activity of antimicrobial peptides is usually associated with strong 431 hemolytic activity and cytotoxicity, and assessment of the in vitro safety of AMP is paramount for 432 further consideration as a potential clinical candidate (Zhang et al. 2024). In this study, our results 433 showed that GmAMP showed little cytotoxicity and low hemolytic effect. Although some cytotoxicity 434



and hemolytic activity were observed at higher concentrations, considering the MIC value of GmAMP 435 was 25 µM (Table 1), which was much lower than its cytotoxicity concentration, GmAMP safety is 436 also guaranteed under the premise of ensuring its activity. However, the potential toxicity of GmAMP 437 to other mammalian cells remains to be studied. 438 Cytotoxicity and hemolytic assays confirmed the safe and effective dosage range of GmAMP, laying 439 the foundation for its application in animal studies. In this study, the therapeutic efficacy of GmAMP 440 was tested in vivo using the Galleria mellonella larvae infection model, which showed a significant 441 improvement in survival. GmAMP treatment significantly reduced the fungal burden of Galleria 442 mellonella larvae in vivo, and these findings suggest that GmAMP may exhibit a strong safety and 443 certain therapeutic potential. 444

CONCLUSIONS

445

This work describes the antifungal activity and mechanism of antimicrobial peptide GmAMP 446 and therapeutic efficacy in vivo. GmAMP possesses potent antimicrobial activity, anti-biofilm 447 formation, and eradication ability, and may play an antimicrobial role by disrupting the structure 448 of fungal cytomembrane. Here, GmAMP displays low cytotoxicity and low hemolytic activity in 449 vitro experiments. Furthermore, GmAMP exhibits a therapeutic effect against fluconazole-450 resistant C. tropical infection and reduces the number of fungi in vivo. These properties make 451 GmAMP a potential treatment for fluconazole-resistant C. tropical infection, which is worthy of 452 further optimization and development. In addition, GmAMP offers more possibilities for the 453 clinical application of antimicrobial peptides for safety and therapeutic efficacy in the 454 development of drug resistance. 455



456 ADDITIONAL INFORMATION AND DECLARATIONS

457 Funding

- This research received funding from National Natural Science Foundation of China
- 459 (No.81760647、82360700)、Science and Technology Planning Project of Guizhou Province
- 460 (ZK[2022] general project 345). Excellent Young Talents Plan of Guizhou Medical University
- (No. [2021]104) and Guizhou Key Laboratory (ZDSYS[2023]004). The funders had no role in
- study design, data collection and analysis, decision to publish, or preparation of the manuscript.

463 Grant Disclosures

- The following grant information was disclosed by the authors:
- National Natural Science Foundation of China: No.81760647 No.82360700
- Science and Technology Planning Project of Guizhou Province: ZK[2022] general project 345
- Excellent Young Talents Plan of Guizhou Medical University: No. [2021]104
- 468 Guizhou Key Laboratory: ZDSYS[2023]004

Competing Interests

The authors declare there are no competing interests.

471 **Author Contributions**

- Ruxia Cai conceived and designed the experiments, performed the experiments, analyzed
- the data, prepared figures and/or tables, authored or reviewed drafts of the article, and
- approved the final draft.
- Na Zhao conceived and designed the experiments, performed the experiments, prepared
- figures and/or tables, authored or reviewed drafts of the article, and approved the final draft.



477	•	Chaoqin Sun performed the experiments, analyzed the data, prepared figures and/or tables,
478		and approved the final draft.

- Mingjiao Huang performed the experiments, prepared figures and/or tables, and approved
 the final draft.
- Zhenlong Jiao performed the experiments, analyzed the data, and approved the final draft.
- Jian Peng performed the experiments, prepared figures and/or tables, and approved the final
 draft.
- Jin Zhang analyzed the data, prepared figures and/or tables, and approved the final draft.
- Guo Guo conceived and designed the experiments, authored or reviewed drafts of the
 article, explore experimental procedures and supervise the experiment, and approved the
 final draft.

488 Data Availability

- The following information was supplied regarding data availability:
- The raw measurements are available in the Supplemental Files.

491 **Supplemental Information**

Supplemental information for this article can be found in supplemental files.

493

494

REFERENCES

- Aguiar FLL, Santos NC, de Paula Cavalcante CS, Andreu D, Baptista GR, and Gonçalves S. 2020. Antibiofilm Activity on Candida albicans and Mechanism of Action on Biomembrane Models of the Antimicrobial Peptide Ctn[15-34]. *Int J Mol Sci* 21. http://dx.org/10.3390/ijms21218339
- Alfaro-Vargas P, Bastos-Salas A, Muñoz-Arrieta R, Pereira-Reyes R, Redondo-Solano M, Fernández J, Mora-Villalobos A, and López-Gómez JP. 2022. Peptaibol Production and Characterization from Trichoderma asperellum and Their Action as



500	Biofungicide. J Fungi (Basel) 8. http://dx.org/10.3390/jof8101037			
501	Badiee P, Boekhout T, Haddadi P, Mohammadi R, Ghadimi-Moghadam A, Soltani J, Zarei Mahmoudabadi A, Ayatollahi Mousavi			
502	SA, Najafzadeh MJ, Diba K, Salimi-Khorashad AR, Amin Shahidi M, Ghasemi F, and Jafarian H. 2022. Epidemiolog			
503	and Antifungal Susceptibility of Candida Species Isolated from 10 Tertiary Care Hospitals in Iran. Microbiol Species			
504	10:e0245322. http://dx.org/10.1128/spectrum.02453-22			
505	Bezerra LP, Freitas CDT, Silva AFB, Amaral JL, Neto NAS, Silva RGG, Parra ALC, Goldman GH, Oliveira JTA, Mesquita FP,			
506	and Souza PFN. 2022. Synergistic Antifungal Activity of Synthetic Peptides and Antifungal Drugs against Candida			
507	albicans and C. parapsilosis Biofilms. Antibiotics (Basel) 11. http://dx.org/10.3390/antibiotics11050553			
508	Boparai JK, and Sharma PK. 2020. Mini Review on Antimicrobial Peptides, Sources, Mechanism and Recent Applications. Protein			
509	Pept Lett 27:4-16. http://dx.org/10.2174/0929866526666190822165812			
510	Buda De Cesare G, Cristy SA, Garsin DA, and Lorenz MC. 2020. Antimicrobial Peptides: a New Frontier in Antifungal Therapy.			
511	mBio 11. http://dx.org/10.1128/mBio.02123-20			
512	Chai LY, Denning DW, and Warn P. 2010. Candida tropicalis in human disease. Crit Rev Microbiol 36:282-298.			
513	http://dx.org/10.3109/1040841x.2010.489506			
514	Chandra J, and Mukherjee PK. 2015. Candida Biofilms: Development, Architecture, and Resistance. Microbiol Spectr 3.			
515	http://dx.org/10.1128/microbiolspec.MB-0020-2015			
516	Chiramba CK, Möller DS, Lorenz CD, Chirombo RR, Mason AJ, Bester MJ, and Gaspar ARM. 2024. Tryptophan End-Tagging			
517	Confers Antifungal Activity on a Tick-Derived Peptide by Triggering Reactive Oxygen Species Production. ACS Omega			
518	9:15556-15572. http://dx.org/10.1021/acsomega.4c00478			
519	CLSI. Clinical and Laboratory Standards Institute; 2023. Performance Standards for Antimicrobial Susceptibility Testing.			
520	Contreras Martínez OI, Angulo Ortíz A, and Santafé Patiño G. 2022. Mechanism of Antifungal Action of Monoterpene			
521	Isoespintanol against Clinical Isolates of Candida tropicalis. <i>Molecules</i> 27. http://dx.org/10.3390/molecules27185808			
522	D'Auria FD, Casciaro B, De Angelis M, Marcocci ME, Palamara AT, Nencioni L, and Mangoni ML. 2022. Antifungal Activity of			
523	the Frog Skin Peptide Temporin G and Its Effect on Candida albicans Virulence Factors. Int J Mol Sci 23.			
524	http://dx.org/10.3390/ijms23116345			
525	de Oliveira AS, de Oliveira JS, Kumar R, Silva FBA, Fernandes MR, Nobre FD, Costa ADC, Albuquerque P, Sidrim JJC, Rocha			
526	MFG, Santos FA, Srivastava V, Romeiro LAS, and Brilhante RSN. 2023. Antifungal activity of sustainable histone			
527	deacetylase inhibitors against planktonic cells and biofilms of Candida spp. and Cryptococcusneoformans. Med Mycol			
528	61. http://dx.org/10.1093/mmy/myad073			
529	Decker T, Rautenbach M, Khan S, and Khan W. 2024. Antibacterial efficacy and membrane mechanism of action of the Serratia-			
530	derived non-ionic lipopeptide, serrawettin W2-FL10. Microbiol Spectr:e0295223.			
531	http://dx.org/10.1128/spectrum.02952-23			
532	Desai JV, and Mitchell AP. 2015. Candida albicans Biofilm Development and Its Genetic Control. Microbiol Spectr 3.			
533	http://dx.org/10.1128/microbiolspec.MB-0005-2014			
534	Falagas ME, Roussos N, and Vardakas KZ. 2010. Relative frequency of albicans and the various non-albicans Candida spp among			
535	candidemia isolates from inpatients in various parts of the world: a systematic review. Int J Infect Dis 14:e954-966.			
536	http://dx.org/10.1016/j.ijid.2010.04.006			
537	Fan X, Dai RC, Zhang S, Geng YY, Kang M, Guo DW, Mei YN, Pan YH, Sun ZY, Xu YC, Gong J, and Xiao M. 2024. Author			
538	Correction: Tandem gene duplications contributed to high-level azole resistance in a rapidly expanding Candida tropicalis			
539	population. Nat Commun 15:587. http://dx.org/10.1038/s41467-024-44825-y			
540	Fan X, Tsui CKM, Chen X, Wang P, Liu ZJ, and Yang CX. 2023. High prevalence of fluconazole resistant Candida tropicalis			



541	among candiduria samples in China: An ignored matter of concern. Front Microbiol 14:1125241.		
542	http://dx.org/10.3389/fmicb.2023.1125241		
543	Fernandes KE, Weeks K, and Carter DA. 2020. Lactoferrin Is Broadly Active against Yeasts and Highly Synergistic wire		
544	Amphotericin B. Antimicrob Agents Chemother 64. http://dx.org/10.1128/aac.02284-19		
545	Fernández de Ullivarri M, Arbulu S, Garcia-Gutierrez E, and Cotter PD. 2020. Antifungal Peptides as Therapeutic Agents. From		
546	Cell Infect Microbiol 10:105. http://dx.org/10.3389/fcimb.2020.00105		
547	Fisher MC, and Denning DW. 2023. The WHO fungal priority pathogens list as a game-changer. Nat Rev Microbiol 21:211-212.		
548	http://dx.org/10.1038/s41579-023-00861-x		
549	Hu N, Mo XM, Xu SN, Tang HN, Zhou YH, Li L, and Zhou HD. 2022. A novel antimicrobial peptide derived from human BPIFA		
550	protein protects against Candida albicans infection. Innate Immun 28:67-78. http://dx.org/10.1177/17534259221080543		
551	Huang Y, Fujii K, Chen X, Iwatani S, Chibana H, Kojima S, and Kajiwara S. 2020. Fungal NOX is an essential factor for induction		
552	of TG2 in human hepatocytes. Med Mycol 58:679-689. http://dx.org/10.1093/mmy/myz105		
553	Jayasinghe JNC, Whang I, and De Zoysa M. 2023. Antifungal Efficacy of Antimicrobial Peptide Octominin II against Candida		
554	albicans. Int J Mol Sci 24. http://dx.org/10.3390/ijms241814053		
555	Jia C, Zhang J, Zhuge Y, Xu K, Liu J, Wang J, Li L, and Chu M. 2019. Synergistic effects of geldanamycin with fluconazole are		
556	associated with reactive oxygen species in Candida tropicalis resistant to azoles and amphotericin B. Free Radic Res		
557	53:618-628. http://dx.org/10.1080/10715762.2019.1610563		
558	Jin Y, Zhang T, Samaranayake YH, Fang HH, Yip HK, and Samaranayake LP. 2005. The use of new probes and stains for improved		
559	assessment of cell viability and extracellular polymeric substances in Candida albicans biofilms. Mycopathologia		
560	159:353-360. http://dx.org/10.1007/s11046-004-6987-7		
561	Khamzeh A, Dahlstrand Rudin A, Venkatakrishnan V, Stylianou M, Sanchez Klose FP, Urban CF, Björnsdottir H, Bylund J, and		
562	Christenson K. 2023. High levels of short chain fatty acids secreted by Candida albicans hyphae induce neutrophil		
563	chemotaxis via Free Fatty Acid Receptor 2. J Leukoc Biol. http://dx.org/10.1093/jleuko/qiad146		
564	Kodedová M, Valachovič M, Csáky Z, and Sychrová H. 2019. Variations in yeast plasma-membrane lipid composition affect		
565	killing activity of three families of insect antifungal peptides. Cell Microbiol 21:e13093. http://dx.org/10.1111/cmi.1309		
566	Lee JK, Park S, Kim YM, Guk T, Choi JK, Kim JY, Lee MY, Jang MK, and Park SC. 2022. Antifungal and Anti-Inflammatory		
567	Activities of PS1-2 Peptide against Fluconazole-Resistant Candida albicans. Antibiotics (Basel) 11.		
568	http://dx.org/10.3390/antibiotics11121779		
569	Lee Y, Puumala E, Robbins N, and Cowen LE. 2021. Antifungal Drug Resistance: Molecular Mechanisms in Candida albicans and		
570	Beyond. Chem Rev 121:3390-3411. http://dx.org/10.1021/acs.chemrev.0c00199		
571	Li R, Zhao J, Huang L, Yi Y, Li A, Li D, Tao M, and Liu Y. 2020. Antimicrobial peptide CGA-N12 decreases the Candida tropicalis		
572	mitochondrial membrane potential via mitochondrial permeability transition pore. Biosci Rep 40.		
573	http://dx.org/10.1042/bsr20201007		
574	Liu Y, Chen Z, Li J, Zhu Z, Pang S, Xu J, and Wu J. 2022. Extensive Diversity and Prevalent Fluconazole Resistance among		
575	Environmental Yeasts from Tropical China. Genes (Basel) 13. http://dx.org/10.3390/genes13030444		
576	Lochenie C, Duncan S, Zhou Y, Fingerhut L, Kiang A, Benson S, Jiang G, Liu X, Mills B, and Vendrell M. 2024. Photosensitizer-		
577	Amplified Antimicrobial Materials for Broad-Spectrum Ablation of Resistant Pathogens in Ocular Infections. Adv		
578	Mater:e2404107. http://dx.org/10.1002/adma.202404107		
579	Ma H, Zhao X, Yang L, Su P, Fu P, Peng J, Yang N, and Guo G. 2020. Antimicrobial Peptide AMP-17 Affects Candida albicans		
580	by Disrupting Its Cell Wall and Cell Membrane Integrity. Infect Drug Resist 13:2509-2520.		
581	http://dx.org/10.2147/idr.S250278		



582 McCarthy MW, and Walsh TJ. 2017. Drug development challenges and strategies to address emerging and resistant fungal 583 pathogens. Expert Rev Anti Infect Ther 15:577-584. http://dx.org/10.1080/14787210.2017.1328279 Melo AKV, da Nóbrega Alves D, Gomes da Costa PCQ, Lopes SP, de Sousa DP, Guerra FQS, Sobral MV, Gomes Moura AP, 584 585 Scotti L, and de Castro RD. 2024. Antifungal Activity, Mode of Action, and Cytotoxicity of 4-chlorobenzyl p-coumarate: 586 a Promising New Molecule. Chem Biodivers: e202400330. http://dx.org/10.1002/cbdv.202400330 587 Mulukutla A, Shreshtha R, Kumar Deb V, Chatterjee P, Jain U, and Chauhan N. 2024. Recent advances in antimicrobial peptidebased therapy. Bioorg Chem 145:107151. http://dx.org/10.1016/j.bioorg.2024.107151 588 589 Pappas PG, Kauffman CA, Andes DR, Clancy CJ, Marr KA, Ostrosky-Zeichner L, Reboli AC, Schuster MG, Vazquez JA, Walsh 590 TJ, Zaoutis TE, and Sobel JD. 2016. Clinical Practice Guideline for the Management of Candidiasis: 2016 Update by the 591 Infectious Diseases Society of America. Clin Infect Dis 62:e1-50. http://dx.org/10.1093/cid/civ933 592 Perrone GG, Tan SX, and Dawes IW. 2008. Reactive oxygen species and yeast apoptosis. Biochim Biophys Acta 1783:1354-1368. http://dx.org/10.1016/j.bbamcr.2008.01.023 593 594 Personne H, Paschoud T, Fulgencio S, Baeriswyl S, Köhler T, van Delden C, Stocker A, Javor S, and Reymond JL. 2023. To Fold 595 or Not to Fold: Diastereomeric Optimization of an α-Helical Antimicrobial Peptide. J Med Chem 66:7570-7583. 596 http://dx.org/10.1021/acs.jmedchem.3c00460 597 Sasani E, Khodavaisy S, Rezaie S, Salehi M, and Yadegari MH. 2021. The relationship between biofilm formation and mortality 598 Candida tropicalis candidemia. Microb Pathog 155:104889. 599 http://dx.org/10.1016/j.micpath.2021.104889 600 Shaban S, Patel M, and Ahmad A. 2024. Antifungal activity of human antimicrobial peptides targeting apoptosis in Candida auris. J Med Microbiol 73. http://dx.org/10.1099/jmm.0.001835 601 602 Taveira GB, de Oliveira Mello É, Simão T, Cherene MB, de Oliveira Carvalho A, Muzitano MF, Lassounskaia E, Pireda S, de 603 Castro Miguel E, Basso LGM, Da Cunha M, da Motta OV, and Gomes VM. 2022. A new bioinspired peptide on defensin 604 from C. annuum fruits: Antimicrobial activity, mechanisms of action and therapeutical potential. Biochim Biophys Acta 605 Gen Subj 1866:130218. http://dx.org/10.1016/j.bbagen.2022.130218 Thomas-Rüddel DO, Schlattmann P, Pletz M, Kurzai O, and Bloos F. 2022. Risk Factors for Invasive Candida Infection in Critically 606 607 Ill Patients: A Systematic Review and Meta-analysis. Chest 161:345-355. http://dx.org/10.1016/j.chest.2021.08.081 608 Torres R, Barreto-Santamaría A, Arévalo-Pinzón G, Firacative C, Gómez BL, Escandón P, Patarroyo MA, and Muñoz JE. 2023. 609 In Vitro Antifungal Activity of Three Synthetic Peptides against Candida auris and Other Candida Species of Medical 610 Importance. Antibiotics (Basel) 12. http://dx.org/10.3390/antibiotics12081234 611 Tsay SV, Mu Y, Williams S, Epson E, Nadle J, Bamberg WM, Barter DM, Johnston HL, Farley MM, Harb S, Thomas S, Bonner 612 LA, Harrison LH, Hollick R, Marceaux K, Mody RK, Pattee B, Shrum Davis S, Phipps EC, Tesini BL, Gellert AB, 613 Zhang AY, Schaffner W, Hillis S, Ndi D, Graber CR, Jackson BR, Chiller T, Magill S, and Vallabhaneni S. 2020. Burden 614 of Candidemia in the United States, 2017. Clin Infect Dis 71:e449-e453. http://dx.org/10.1093/cid/ciaa193 615 Tseng KY, Liao YC, Chen FC, Chen FJ, and Lo HJ. 2022. A predominant genotype of azole-resistant Candida tropicalis clinical 616 strains. Lancet Microbe 3:e646. http://dx.org/10.1016/s2666-5247(22)00179-3 617 Venkatesh M, Barathi VA, Goh ETL, Anggara R, Fazil M, Ng AJY, Harini S, Aung TT, Fox SJ, Liu S, Yang L, Barkham TMS, 618 Loh XJ, Verma NK, Beuerman RW, and Lakshminarayanan R. 2017. Antimicrobial Activity and Cell Selectivity of 619 Synthetic and Biosynthetic Cationic Polymers, Antimicrob Agents Chemother 61, http://dx.org/10.1128/aac.00469-17 Wang Y, Fan X, Wang H, Kudinha T, Mei YN, Ni F, Pan YH, Gao LM, Xu H, Kong HS, Yang Q, Wang WP, Xi HY, Luo YP, Ye 620 621 LY, and Xiao M. 2021. Continual Decline in Azole Susceptibility Rates in Candida tropicalis Over a 9-Year Period in

China. Front Microbiol 12:702839. http://dx.org/10.3389/fmicb.2021.702839



623	World Health Organization (WHO) ARDA, Control of Neglected Tropical Diseases (NTD), Global Coordination and Partnership
624	(GCP). 2022. WHO fungal priority pathogens list to guide research, development and public health action.

- Zhang H, Chen Q, Xie J, Cong Z, Cao C, Zhang W, Zhang D, Chen S, Gu J, Deng S, Qiao Z, Zhang X, Li M, Lu Z, and Liu R.
 2023. Switching from membrane disrupting to membrane crossing, an effective strategy in designing antibacterial polypeptide. *Sci Adv* 9:eabn0771. http://dx.org/10.1126/sciadv.abn0771
- Zhang H, Zhang S, Wang P, Qin Y, and Wang H. 2017. Forecasting of particulate matter time series using wavelet analysis and
 wavelet-ARMA/ARIMA model in Taiyuan, China. J Air Waste Manag Assoc 67:776-788.
 http://dx.org/10.1080/10962247.2017.1292968
- Zhang J, Yang L, Tian Z, Zhao W, Sun C, Zhu L, Huang M, Guo G, and Liang G. 2022. Large-Scale Screening of Antifungal
 Peptides Based on Quantitative Structure-Activity Relationship. ACS Med Chem Lett 13:99-104.
 http://dx.org/10.1021/acsmedchemlett.1c00556
- Zhang LM, Zhou SW, Huang XS, Chen YF, Mwangi J, Fang YQ, Du T, Zhao M, Shi L, and Lu QM. 2024. Blap-6, a Novel
 Antifungal Peptide from the Chinese Medicinal Beetle Blaps rhynchopetera against Cryptococcus neoformans. *Int J Mol Sci* 25. http://dx.org/10.3390/ijms25105336
- Zhou Y, Meng X, Chen F, Xiong M, Zhang W, and Wang KJ. 2023. Newly Discovered Antimicrobial Peptide Scyampcin(44-63)
 from Scylla paramamosain Exhibits a Multitargeted Candidacidal Mechanism In Vitro and Is Effective in a Murine Model
 of Vaginal Candidiasis. Antimicrob Agents Chemother 67:e0002223. http://dx.org/10.1128/aac.00022-23
- Zhu X, Jin F, Yang G, Zhuang T, Zhang C, Zhou H, Niu X, Wang H, and Wu D. 2024. Mitochondrial Protease Oct1p Regulates
 Mitochondrial Homeostasis and Influences Pathogenicity through Affecting Hyphal Growth and Biofilm Formation
 Activities in Candida albicans. *J Fungi (Basel)* 10. http://dx.org/10.3390/jof10060391
- Zou K, Yin K, Ren S, Zhang R, Zhang L, Zhao Y, and Li R. 2024. Activity and mechanism of action of antimicrobial peptide ACPs
 against Candida albicans. *Life Sci*:122767. http://dx.org/10.1016/j.lfs.2024.122767
- Zuza-Alves DL, Silva-Rocha WP, and Chaves GM. 2017. An Update on Candida tropicalis Based on Basic and Clinical
 Approaches. Front Microbiol 8:1927. http://dx.org/10.3389/fmicb.2017.01927





Table 1(on next page)

Antifungal activity of GmAMP.

The determination of the antifungal activity of GmAMP against four strains of *C. tropicalis*.



Table 1:

- 2 Antifungal activity of GmAMP.
- 3 The determination of the antifungal activity of GmAMP against four strains of *C. tropicalis*.

Strains	MIC (μM)	
	GmAMP	Fluconazole
Fluconazole-resistant <i>C. tropicalis</i> 4252	25	>3343
Fluconazole-resistant <i>C. tropicalis</i> 4171	50	>3343
Fluconazole-resistant <i>C. tropicalis</i> 6984	50	>3343
Fluconazole-resistant <i>C. tropicalis</i> 8402	50	>3343
C. tropicalis ATCC 20962	12	13

4



Physicochemical properties of GmAMP.

(A) Heliquest software (https://heliquest. ipmc.cnrs.fr/) was used to draw the spiral wheel diagram, positively charged amino acids are indicated in blue, uncharged polar residues are shown in purple the red 'N' represents the starting position and the arrow represents the hydrophobic moment. (B) The structure of GmAMP was predicated by AlphFold2. (C) The physical and chemical properties of GmAMP were analyzed via the Expasy ProtParam website (http://web.expasy.org/protparam/).



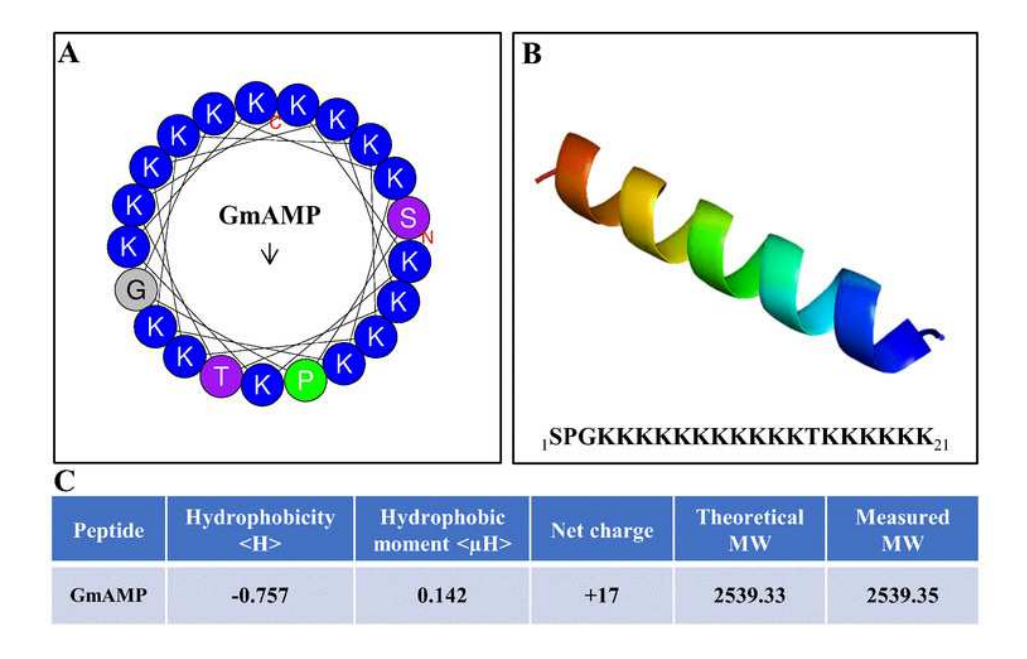


Figure 1 Physicochemical properties of GmAMP. (A) Heliquest software (https://heliquest. ipmc.cnrs.fr/) was used to draw the spiral wheel diagram, positively charged amino acids are indicated in blue, uncharged polar residues are shown in purple, the red 'N' represents the starting position and the arrow represents the hydrophobic moment. (B) The structure of GmAMP was predicated by AlphFold2. (C) The physical and chemical properties of GmAMP were analyzed via the Expasy ProtParam website (http://web.expasy.org/protparam/).



Effect of GmAMP on the growth of fluconazole-resistant *C. tropicalis*.

(A) Growth kinetics of fluconazole-resistant *C. tropicalis*. (B) Time-killing kinetics of fluconazole-resistant *C. tropicalis*. (C) The transformation from yeast phase to mycelial phase of fluconazole-resistant *C. tropicalis*. Scale bar, 25 µm.



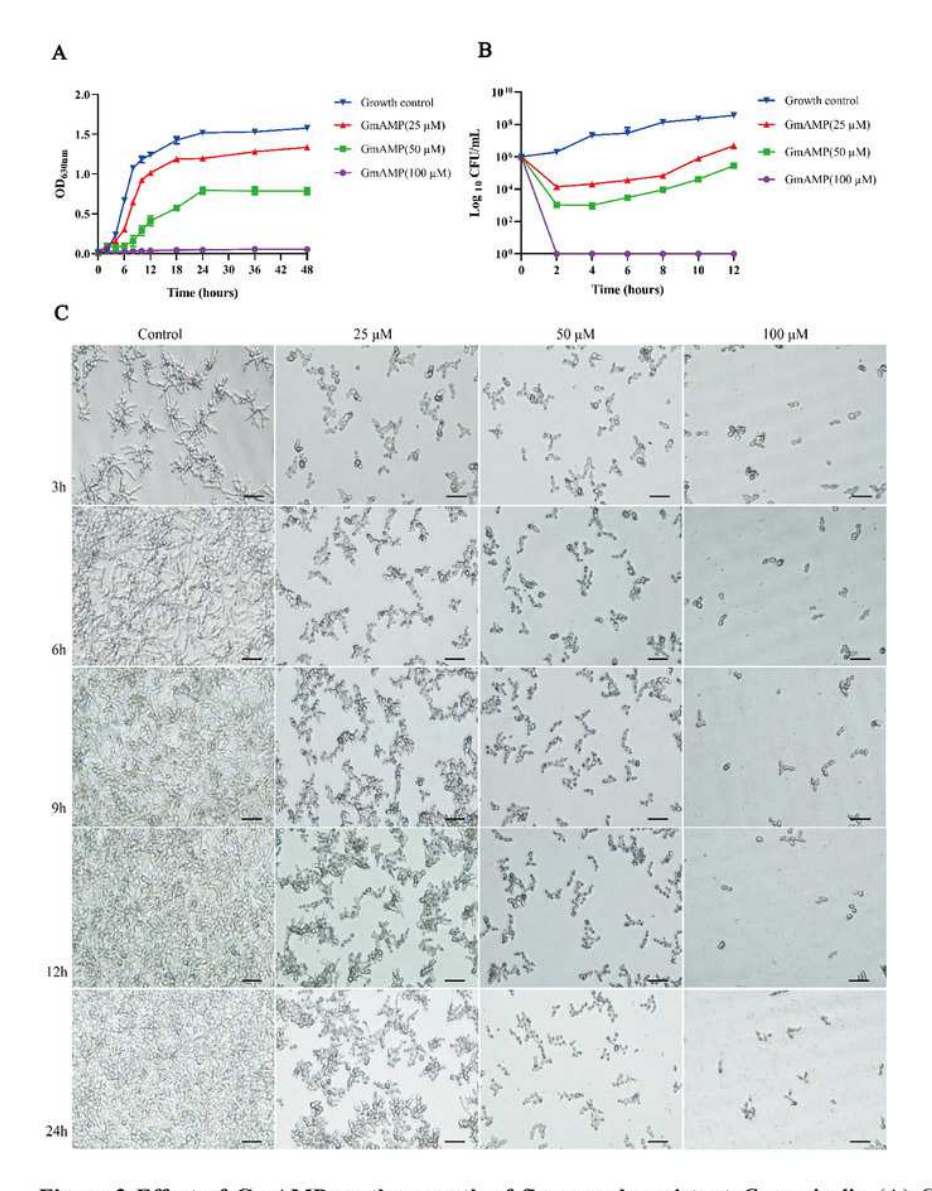


Figure 2 Effect of GmAMP on the growth of fluconazole-resistant *C. tropicalis*. (A) Growth kinetics of fluconazole-resistant *C. tropicalis*. (B) Time-killing kinetics of fluconazole-resistant *C. tropicalis*. (C) The transformation from yeast phase to mycelial phase of fluconazole-resistant *C. tropicalis*. Scale bar, 25 μm.



Effect of GmAMP on the biofilm of fluconazole-resistant C. tropicalis.

Inhibition (A) and eradication (B) effects of fluconazole-resistant *C. tropicalis* biofilms treated with GmAMP at different concentrations observed by confocal laser scanning microscopy. Images obtained by live/dead staining (SYTO 9, green; PI, red). Scale bar, 20 µm. The activity level of biofilm under different concentrations of GmAMP was determined by the XTT reduction method (C and D), and the colorimetric absorbance was measured at OD490nm. The error bar represents the standard deviation of the three independent experiments. ***P < 0.001 compared with the control group.



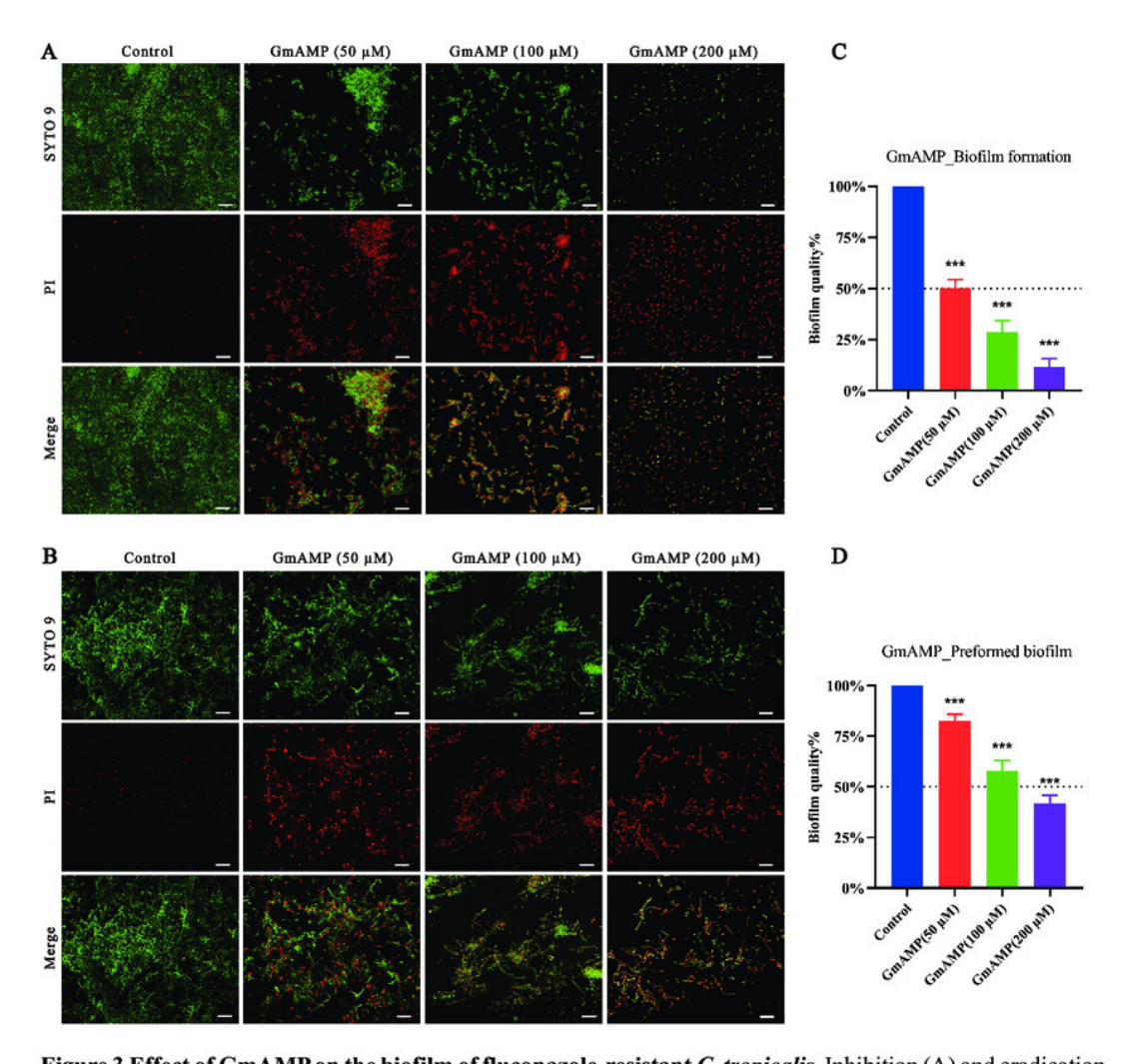


Figure 3 Effect of GmAMP on the biofilm of fluconazole-resistant C. tropicalis. Inhibition (A) and eradication (B) effects of fluconazole-resistant C. tropicalis biofilms treated with GmAMP at different concentrations observed by confocal laser scanning microscopy. Images obtained by live/dead staining (SYTO 9, green; PI, red). Scale bar, 20 μ m. The activity level of biofilm under different concentrations of GmAMP was determined by the XTT reduction method (C and D), and the colorimetric absorbance was measured at OD_{490nm}. The error bar represents the standard deviation of the three independent experiments. ***P < 0.001 compared with the control group.

Effects of GmAMP cell morphology and cell membranes of fluconazole-resistant *C. tropicalis*.

The control group (A) and GmAMP group treated with 100 μ M (B) of fluconazole-resistant *C. tropicalis* morphological images by scanning electron microscopy. (C) Cell membrane permeability of GmAMP on the fluconazole-resistant *C. tropicalis* was determined by flow cytometry, and with SYTO 9 and PI as pore formation mechanism marker. (D) DiSC3(5) was used to detect the cell membrane depolarization of fluconazole-resistant *C. tropicalis*. (E) The ROS-induced accumulation of DCFH-DA is a pore formation mechanism marker



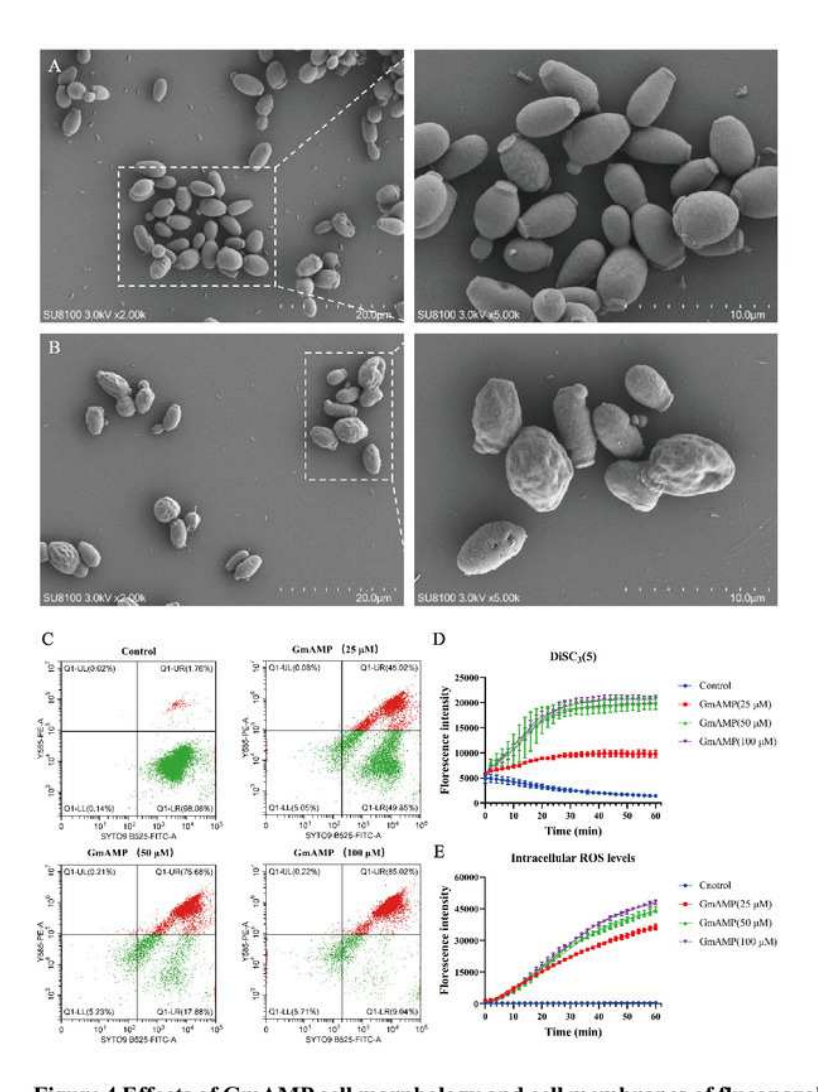


Figure 4 Effects of GmAMP cell morphology and cell membranes of fluconazole-resistant *C. tropicalis*. The control group (A) and GmAMP group treated with 100 μM (B) of fluconazole-resistant *C. tropicalis* morphological images by scanning electron microscopy. (C) Cell membrane permeability of GmAMP on the fluconazole-resistant *C. tropicalis* was determined by flow cytometry, and with SYTO 9 and PI as pore formation mechanism marker. (D) DiSC₃(5) was used to detect the cell membrane depolarization of fluconazole-resistant *C. tropicalis*. (E) The ROS-induced accumulation of DCFH-DA is a pore formation mechanism marker.



The hemolytic and cytotoxicity effects of GmAMP.

(A) The cytotoxicity of GmAMP against RAW 264.7 cells. (B) The hemolysis rate of 2% human red blood cells.



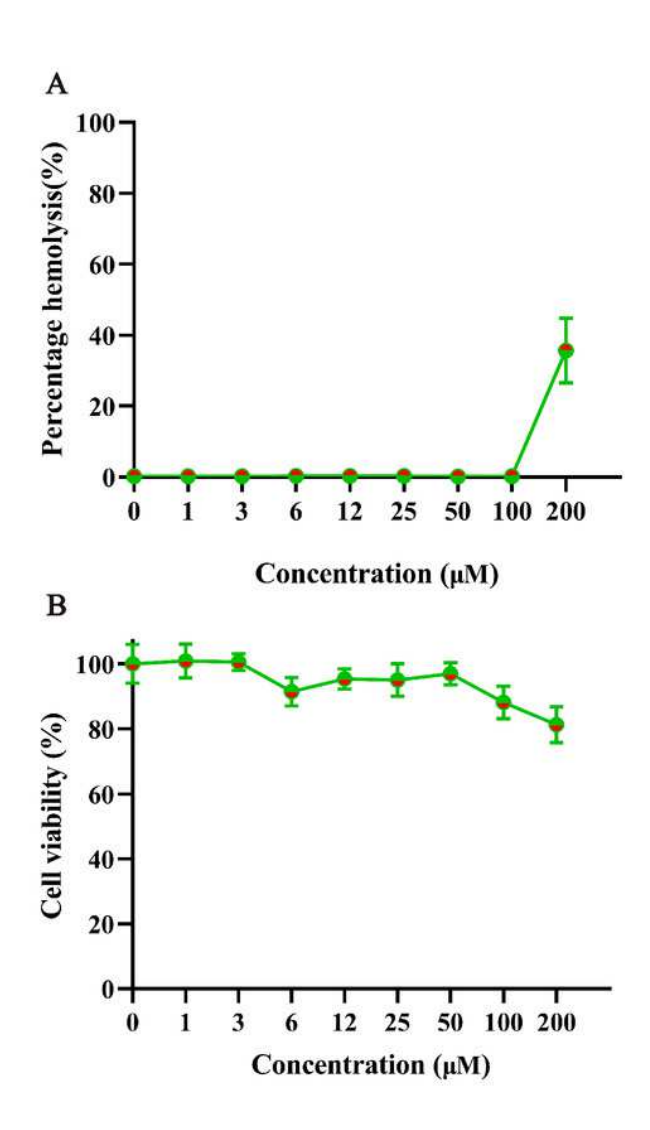


Figure 5 The hemolytic and cytotoxicity effects of GmAMP. (A) The cytotoxicity of GmAMP against RAW 264.7 cells. (B) The hemolysis rate of 2% human red blood cells.



In vivo toxicity and therapeutic activity of GmAMP in the G. mellonella model.

(A) Schematic diagram of the GmAMP treatment. (B) The toxicity of GmAMP in *G. mellonella* larvae model. (C) Survival of larvae after treatment with GmAMP. (D) Fungal burden of larvae after treatment with GmAMP. *P < 0.05; ***P < 0.001 compared with the group of fluconazole-resistant *C. tropicalis* + PBS.



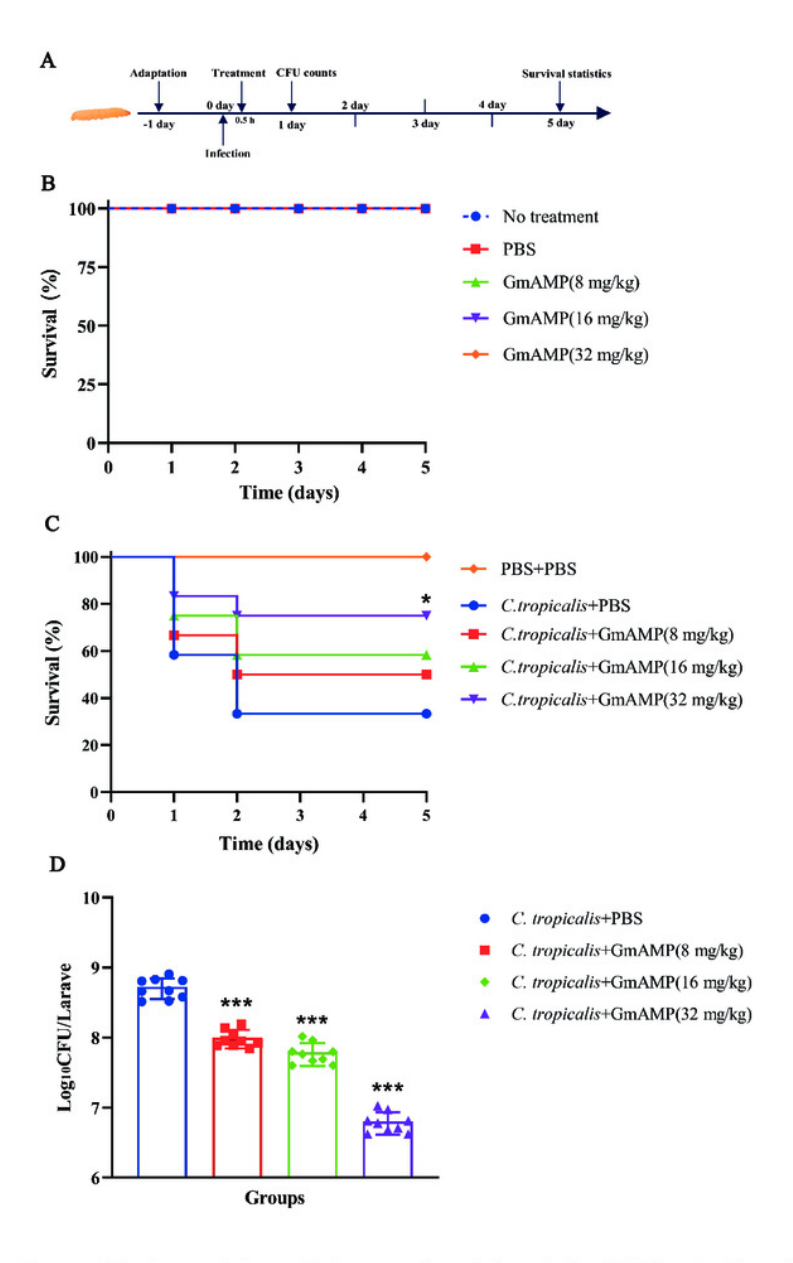


Figure 6 In vivo toxicity and therapeutic activity of GmAMP in the G. mellonella model. (A) Schematic diagram of the GmAMP treatment. (B) The toxicity of GmAMP in G. mellonella larvae model. (C) Survival of larvae after treatment with GmAMP. (D) Fungal burden of larvae after treatment with GmAMP. *P < 0.05; ***P < 0.001 compared with the group of fluconazole-resistant C. tropicalis + PBS.